


RESEARCH ARTICLE

Open Access



Fast, accessible and reliable method for elemental analysis of metals in solution by ED-XRF spectroscopy

Filipe M. J. Figueiredo¹, José M. Carretas^{2,3}, João P. Leal^{2,3} and José M. Sardinha^{1,3*} 

Abstract

The measurement of metals in solution is usually performed using inductive coupled plasma hyphenated techniques or atomic absorption. Although very sensitive and accurate, these analytical techniques are quite expensive and do not allow field measurements. The present work takes advantage of energy-dispersive X-ray fluorescence (ED-XRF) ease-of-use features to determine the concentration of rare earth elements (Y, Pr, Nd, Eu) and others (S, Fe, Ni, Cu, Zn) in aqueous solutions, after appropriate sample treatment. The approach turned out to be a reliable and very convenient procedure for field analysis. The simplicity, speed and reliability of the methodology used combined with the possibility of simultaneous analysis and low cost of the method can be advantageous in industrial context. The approach relies on the suspension of the target solutions in a cellulose matrix that is further converted into a pellet for direct analysis. Calibration curves obtained by regression analysis at 5% significance are shown for a variety of elements (S, Fe, Ni, Cu, Zn, Y, Pr, Nd, Eu) with correlation coefficients between 0.9555 and 0.9980. Higher coefficients of variance were obtained for the calibration of S and Pr due to low sensitivity and the overlapping with the L lines of Nd, respectively. The performed calibrations were not affected by the presence of other analytes in the matrix. Results obtained showed that it is possible to use the proposed methodology to accurately quantify d and f block metals in aqueous solutions by ED-XRF after sequestering the chemical content into a cellulose powder matrix and further processing into a pellet.

Keywords ED-XRF, Field analyses, Metals in solution, Calibrations, Rare earth elements, Pressed pellets

*Correspondence:

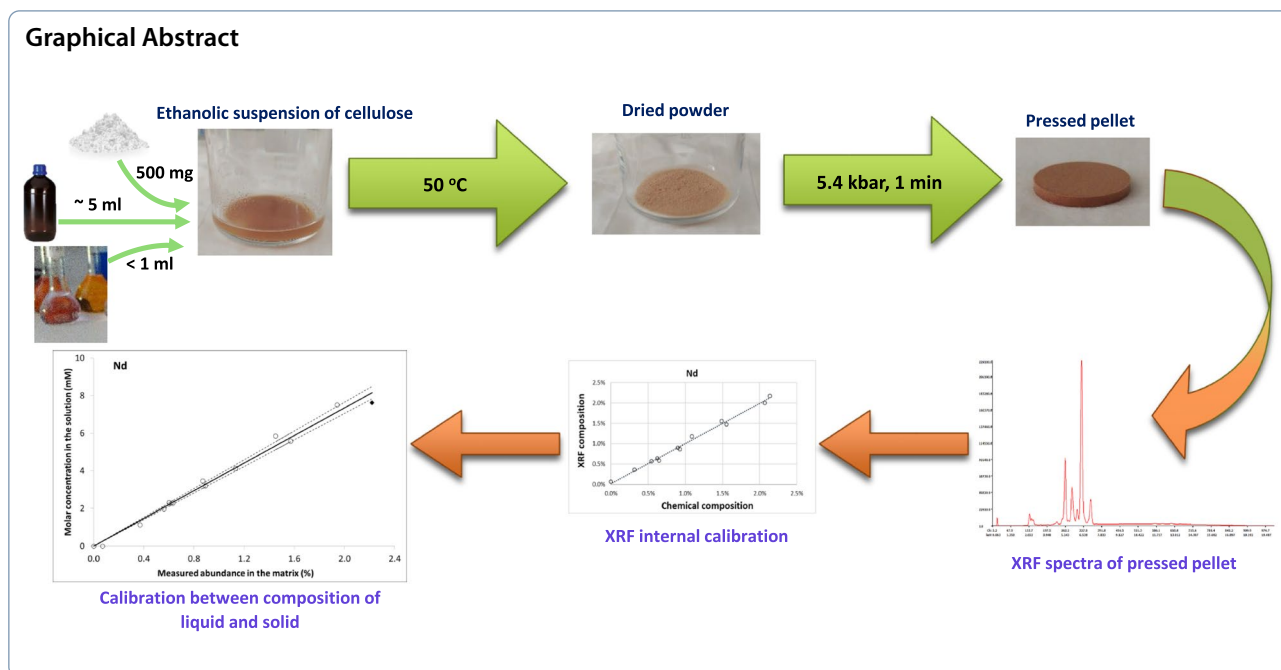
José M. Sardinha

jose.sardinha@tecnico.ulisboa.pt

Full list of author information is available at the end of the article



© The Author(s) 2024. **Open Access** This article is licensed under a Creative Commons Attribution 4.0 International License, which permits use, sharing, adaptation, distribution and reproduction in any medium or format, as long as you give appropriate credit to the original author(s) and the source, provide a link to the Creative Commons licence, and indicate if changes were made. The images or other third party material in this article are included in the article's Creative Commons licence, unless indicated otherwise in a credit line to the material. If material is not included in the article's Creative Commons licence and your intended use is not permitted by statutory regulation or exceeds the permitted use, you will need to obtain permission directly from the copyright holder. To view a copy of this licence, visit <http://creativecommons.org/licenses/by/4.0/>.



Introduction

The aim of elemental analysis is to identify either the elements present within a compound or material or their concentration (Rodrigues et al. 2019; Fiamegos and Calle Guntiñas 2018; Sysoev 2011). Proper metal determination is very important in a wide range of fields, including chemistry (Zhang et al. 2007), chemical engineering (Kejonen et al. 2018), cosmetics (de la Calle et al. 2017), pharmacology (Pinheiro et al. 2020; Rudovica et al. 2014), geology (El-TaHER 2012; Maltsev et al. 2021; Rowe et al. 2012), archaeology (Williams et al. 2020), numismatics (Gentelli 2021), medicine (Pozebon et al. 2017), zoology (Shinn et al. 2000), ecology (Morales et al. 2020; Popp et al. 2010), agriculture (Blotevogel et al. 2019; Maione et al. 2022) and many others (Fiamegos et al. 2020; Perring and Andrey et al. 2018; Perring et al. 2017).

Quantitative analysis of elements in solution is usually performed by inductive coupled plasma hyphenated techniques (mass spectrometry or atomic emission spectroscopy, ICP-MS and ICP-AES, respectively) or atomic absorption spectroscopy (AAS). ICP-based techniques allow the determination of various elements simultaneously (or in series), have good precision, low detection limits and automation of the systems and are available commercially (Skoog et al. 2017). The technique is a standard procedure for chemical composition analysis when aggressive conditions and hazardous chemicals must be used to overcome the difficulty to fully digest some inert matrices (Goswami et al. 2021;

Riding 2021), namely electronic waste (Önal and Binne-mans 2019; Yin et al. 2018). Nevertheless, this approach has high running costs due to the required reagents and gases, auxiliary equipment and procedures (Jin 2016; Rodushkin et al. 2010). Also, daily re-calibration is mandatory which further increases the time to obtain a result. Further, the instruments are not portable, which makes it impossible to carry out measurements in the field. AAS needs a light source for each element, has limited sensitivity and is not capable of simultaneous analysis (Skoog et al. 2017). This technique, including AES (atomic emission spectroscopy) and AFS (atomic fluorescence spectroscopy), can only detect one element at a time, making the analyses very time-consuming. Alternative techniques, such as laser-induced breakdown spectroscopy (LIBS) (Pathak et al. 2012) and spark-induced breakdown spectroscopy (SIBS) (Pinjun et al. 2023), that require a laser are also capable of analysing elemental composition in a similar way as XRF (X-ray fluorescence), being preferred for lighter elements.

Instead, portable energy-dispersive XRF (ED-XRF) portrays the cheapest spectrometer among X-ray fluorescence techniques, maintaining multianalyte measurement capability as well as accuracy (Skoog et al. 2017). Therefore, the technique presents important advantageous features to develop more practical and inexpensive analytical methods. In addition, ED-XRF is suitable for some ppm to percentage (depending on the element), which suits its use to quantify elemental concentrations

in a wide range of compositions. Portable ED-XRF spectrometers are commercially available from various brands constituting an attractive factor for the industry. The technique has proved to be an accurate approach for fieldwork (Rowe et al. 2012; Kalnicky and Singhvi 2001) and industry (Kejonen et al. 2018), namely to analyse solid samples. However, XRF measurements in liquids/solutions require further operational attention to be considered for quantitative analysis. Specifically, special attention should be paid when: (a) using solvents that heavily scatter X-rays, which leads to low sensitivity and poor signal to background ratio (Marguí et al. 2014) and (b) the eventual generation of bubbles in liquid samples, that may lead to incomplete filling of the sample cup bottom affecting measurement reproducibility. Also, there is a risk of leakage and consequent damage of the spectrometer and loss of sample (Moriyama and Morikawa 2017).

Thus, having a simple methodology without the use of other materials, such as sample cups, would be very convenient from the operational point of view, especially in industrial environment where technological resources are usually scarce. Several efforts have been made in the past for the determination of elements in solution, by using some sort of matrix to accommodate the liquid sample, for instance, the simultaneous determination of scandium (III), yttrium (III) and lanthanoid (III) ions from minerals by adding the solution to a special resin (Moriyasu et al. 1991), the analysis of total chromium from dust by adding the solution to cellulose acetate filters (Hurst 1996), or the determination of copper and iron from gasoline using cellulose paper filter (Teixeira et al. 2007). However, these methods usually need mechanical stirring to ensure sample homogeneity, whereas the reduced thickness of the filter has limited adsorption capacity.

Some more complex methodologies have been reported, namely using freeze drying, precipitation of metals, electrodeposition or impregnated membranes (Marguí et al. 2010). A few publications also report the addition of a thickening agent such as gelatine, sucrose or icosane to transform the solution into a “quasi-solid specimen” under vacuum atmosphere (García-Florentino et al. 2017; Marguí et al. 2010; Teixeira et al. 2007). Despite the interest, these methods are complicated to implement, expensive and difficult to ensure homogeneity of the sample. Further, none of these methods has been used for rare earth elements (REE) analysis. In fact, the analysis of REE in solid matrices is not commonly performed, because of lack of proper calibrations. Just more recently, research regarding WEEE (Figueiredo et al. 2024) and geological materials (Akbulut 2014; Rowe et al. 2012) addressed these potentially useful

methodologies. REE has been defined by the EU as critical materials (European Commission 2018; Binnemans et al. 2013). Recycling of REE-rich wastes is very important to accomplish the objectives of circular economy (Ray and Mishra 2023). NdFeB magnets and phosphors have been appointed as important REE-rich components targets (Jha et al. 2016).

In this work, a simple methodology was developed and tested to allow performing elemental analysis on liquid samples, namely containing REE, among others, using a portable ED-XRF spectrometer.

Briefly, the proposed methodology includes: (i) pipetting the liquid solution over cellulose powder, (ii) addition of ethanol and homogenisation, (iii) evaporation and (iv) cold pressing. This simple pretreatment assures sample homogeneity by creating sufficient volume that can be manually stirred. Cellulose, as a transparent material to X-rays, was used as support to sorb the target metal ions. The adopted procedure reduces the concentration of metals in the solid matrix, which decreases the significance of X-ray matrix effects and thus reduces the necessary number of standards to have a precise and linear calibration (Kalnicky and Singhvi 2001). Ethanol was added to ease homogenization and reduce drying time. Further, the methodology is low cost, especially when compared with other reported methods, and, more importantly, is compatible with fieldwork since it can produce accurate results without complex analysis systems that use, for instance, vacuum or helium purges.

Materials and methods

Materials

Ammonium sulphate ((NH₄)₂SO₄, 99%, Ph. Eur, PA-ACS-ISO) was purchased from Panreac. Microcrystalline cellulose was purchased from Acros. Yttrium nitrate hexahydrate (Y(NO₃)₃·6H₂O, 99.8% trace metals basis), praseodymium nitrate hexahydrate (Pr(NO₃)₃·6H₂O, 99.9%), neodymium nitrate hexahydrate (Nd(NO₃)₃·6H₂O, 99.9%), europium nitrate pentahydrate (Eu(NO₃)₃·5H₂O, 99.9% trace metals basis) and zinc nitrate hexahydrate (Zn(NO₃)₂·6H₂O, 99%,) were purchased from Aldrich. Copper(II) nitrate hemipentahydrate (Cu(NO₃)₂·2.5H₂O, 98%) was purchased from Alfa Aesar. Nickel(II) nitrate hexahydrate (Ni(NO₃)₂·6H₂O, 98%, extrapure) was purchased from Scharlau. Ethanol (absolute, 99.5%, for HPLC) was purchased from Fisher.

A Bruker S1 Titan 600 portable (handheld) ED-XRF spectrometer was used to perform the present work, containing a 50 kV X-ray tube with a Rh anode as excitation source and a silicon drift detector (SDD) protected against puncturing by a grid shield. The equipment uses an incidence angle at 45° and a take-off angle at 65°. The collimation of the incident X-ray beam makes the spot

not react with the metals under study and is generally recognized as safe (GRAS). The ethanolic mixture was shaken for 5 min using an orbital agitator and left to dry at 50 °C in an oven with air circulation. The dried powder was homogenized using a glass rod prior to pelletizing. Pellets were prepared using a hydraulic press (7000 kg_f) for 1 min using a 13-mm die set from Aldrich, followed by a slow pressure relief.

XRF measurement

A Bruker S1 Titan 600 ED-XRF spectrometer was positioned vertically over a laboratory bench, with the help of an appropriate support making available the measurement area on top of the equipment, where the primary beam points upwards (Fig. 1) and a shield box stops the X-rays from escaping.

Prepared disc pellets were placed on top of the equipment and measurements performed according with equipment instructions either using manufacturer's pre-installed calibration Geomining with two phases for set A, or the new user-developed calibrations for sets B and C (see Section "XRF specific calibrations").

XRF specific calibrations

Since the XRF equipment used had no calibrations for lanthanoids, as required for measurements in sets B and C, new calibrations were developed and installed on the portable XRF spectrometer, as described elsewhere (Figueiredo et al. 2024). Briefly, calibrations were developed using the



Fig. 1 The Bruker S1 Titan 600 ED-XRF spectrometer positioned vertically over the laboratory bench, with the help of an appropriate support. The shield box is rotated prior to analysis to avoid escape of X-rays

EasyCal™ software, version 2.4.222, part of the Bruker® Toolbox, version 1.6.0.110. Spectra obtained using different operating conditions (tube potential, current intensity, counting time, use of filters) were evaluated and the figure of merit (FOM, Eq. 1) determined. FOM was adapted from the theory of X-ray fluorescence (Jenkins and Vries 1973) and used elsewhere for similar purposes (Potts et al. 1986),

$$\text{FOM} = \sqrt{I_p} - \sqrt{I_{bkg}} \quad (1)$$

in which the I_p refers to the gross intensity at the emission energy of the analyte, and I_{bkg} refers to the intensity of the respective background. FOM was calculated for two key-elements, in different ranges of concentration (Y and Eu for the CRT phosphors, and Pr and Nd for NdFeB magnets). The optimal operating conditions were determined by finding maximum FOM for both elements (Eq. 1), while being aware that different elements may have different optimal conditions of excitation and, thus, the best conditions for one may not suit the other. The K α line was used to analyse sulphur and the transition metals, while L α was used to analyse the lanthanoids.

After introducing the necessary input on the software, the spectra of the disc pellets standards were recorded. For the chosen X-ray line, the most appropriate statistical parameters and corrections (namely matrix effects and overlaps of lines) were chosen in order to minimize the error of the regression model obtained by the software. The development of the spectrometer calibration model for the set B took into consideration the following overlaps of peaks: (i) L α of Pr over Nd L α ; (ii) L α of Nd over Pr L α ; and (iii) K α of Fe over Nd L γ .

For each analyte, a pair of alpha coefficients was obtained by regression analysis using the Bruker software. For the development of the spectrometer calibration model for set C, the overlap of K α of S with the Rh LI line (Rayleigh scattering) was considered. Alpha coefficients were obtained by regression analysis using the software: (i) the element Zn in the calibration for Y and (ii) the elements Zn and Y in the calibration for S. For Zn and Eu, no alpha corrections were computed. At this point, plots of the "compositions" obtained by XRF as a function of the chemical composition of the standards were obtained (see Additional file 1: Figs. S1 and S2 from Online Resource).

Regression analysis

Calibration curves relating the molarity of the solutions and the respective XRF measurements were obtained using linear regression by the least squares method with null y-intercept on Microsoft Excel® (Analysis Tool Pack add-in). The curves fit Eq. 2,

$$C = \beta\omega, \quad (2)$$

with C being the molar concentration in the solution, ω the respective measured concentration in the disc pellet of one analyte and β the slope estimated by the method. Its standard error at 95% confidence $\delta\beta$ was also estimated by the method and multiplied by the corresponding t-Student parameter t . The 95% confidence interval $(\beta \pm \delta\beta t)\omega$ for the regression was plotted along with the linear fit to the experimental data. The coefficients of variance were computed according to Eq. 3,

$$CV = \frac{\delta\beta}{\beta}. \tag{3}$$

Results

For set A, the XRF measurement composition (%) of each disc pellet obtained with the spectrometer (for every chosen element) was plotted against the molar concentration of the metal aqueous solutions to determine the respective correlation (Fig. 2), where dashed lines represent the 95% confidence interval. The composition

was obtained by using the Geomining calibration with the Oxides Method with two phases present in the XRF equipment used. The last phase of this method, which applies a smaller potential and is preferred for lighter elements, did not improve the results and increased noise, therefore being dismissed.

For set B, the optimal conditions for analysis were achieved when using 20 kV and 35 μ A for 60 s. Calibration curves with each data set and a 95% confidence level range are shown in Fig. 3, for Fe, Pr and Nd. In Additional file 1: Fig. S3 from Online Resource, it is observed that the Pr L α line is very close to Nd L α line, and its maximum cannot be observed distinctly in the spectra of some of the standards, therefore making the quantification of praseodymium, which is presented in only small amounts in the pellets (less than 0.3% wt.), more challenging.

For set C, the optimal conditions for analysis were achieved when using 30 kV and 40 μ A for 120 s, while using a 25 μ m Ti filter and a 300 μ m Al filter.

Calibration curves with each data set and a 95% confidence level range are shown in Fig. 4 for S, Zn, Y and

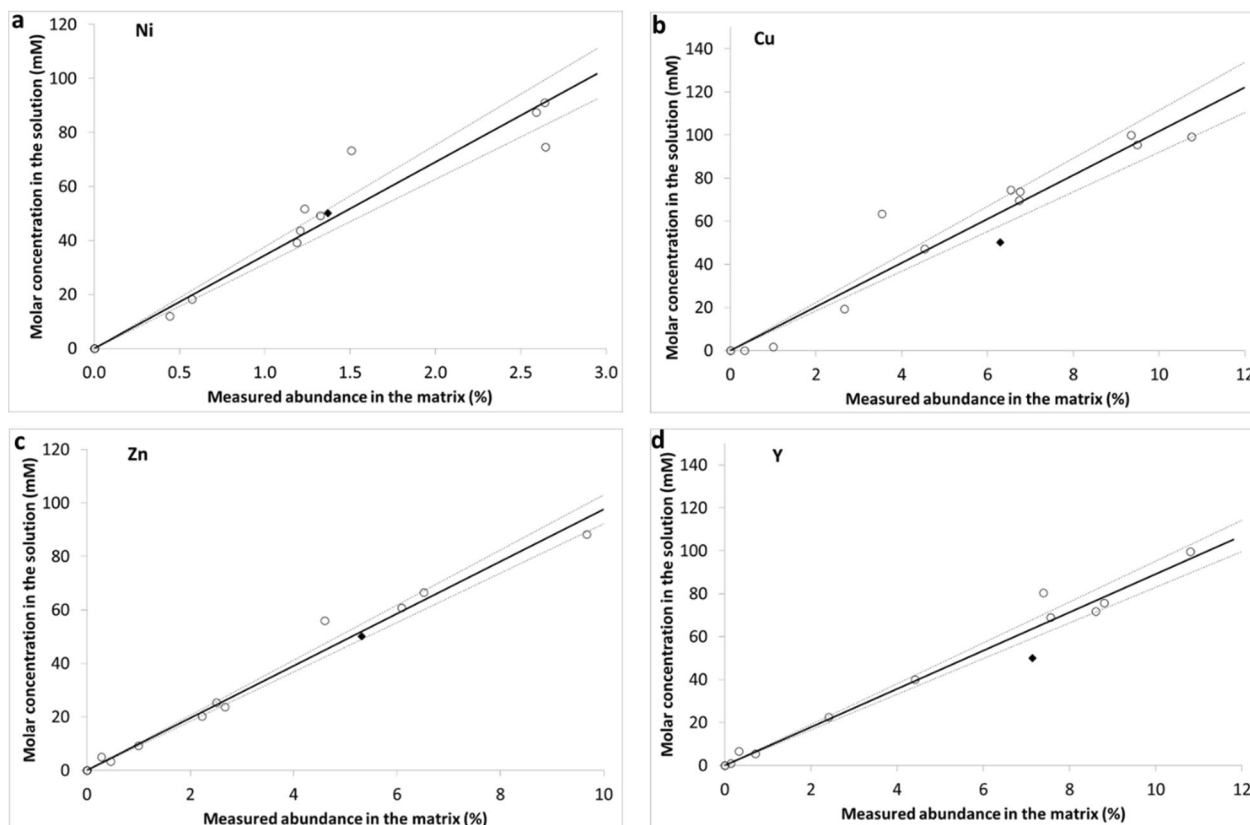


Fig. 2 Correlations obtained between metal concentration in solution and XRF measurements of the pellet, within set A elements (Ni, Cu, Zn and Y). The regression lines follow the equations: **a:** Ni–y/mM = (34.5 ± 1.5)x %, $R^2 = 0.9777$, CV = 4%; **b:** Cu–y/mM = (10.18 ± 0.45)x %, $R^2 = 0.9756$, CV = 4%; **c:** Zn–y/mM = (9.77 ± 0.25)x %, $R^2 = 0.9918$ and a CV = 3%; **d:** Y–y/mM = (8.91 ± 0.28)x %, $R^2 = 0.9875$, CV = 3%. The black diamond in each plot represents the standard that contains only the element of the respective curve

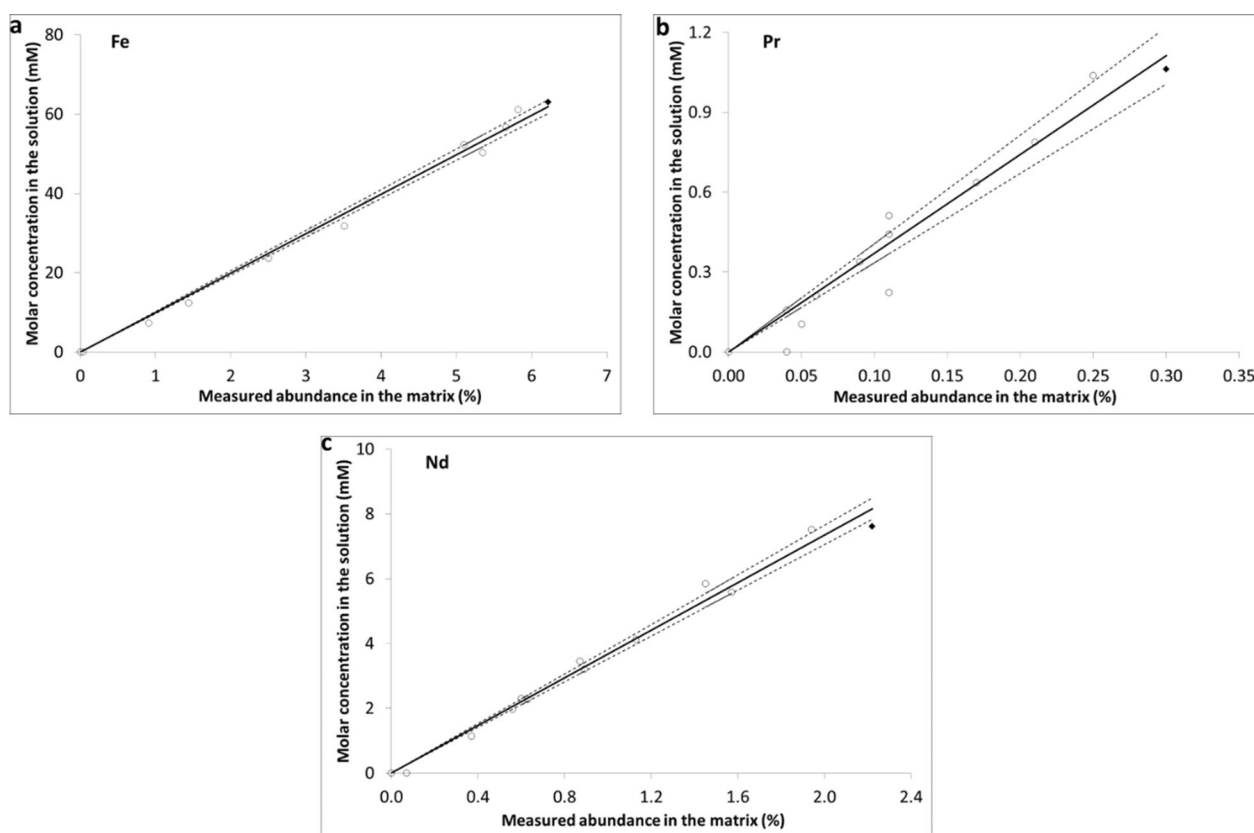


Fig. 3 Correlations obtained between metal concentration in solution and XRF measurements of the pellet, within set B elements (Fe, Pr and Nd). The regression lines follow the equations: **a:** $\text{Fe}-y/\text{mM} = (9.95 \pm 0.13)x \%$, $R^2 = 0.9980$, $\text{CV} = 1\%$; **b:** $\text{Pr}-y/\text{mM} = (3.71 \pm 0.16)x \%$, $R^2 = 0.9772$, $\text{CV} = 4\%$; **c:** $\text{Nd}-y/\text{mM} = (3.676 \pm 0.068)x \%$, $R^2 = 0.9960$ and a $\text{CV} = 2\%$. The black diamond in each plot represents the standard that contains only the element of the respective curve

Eu. Results for sulphur (Fig. 4a) revealed slightly higher statistical dispersion (coefficient of variance 6%). In fact, sulphur is a light element, possessing therefore a lower sensitivity in ED-XRF, and can also easily be hidden by scattered continuous *bremsstrahlung* radiation. It is noteworthy that standards spectra from this matrix (Additional file 1: Fig. S4 from Online Resource) exhibit a higher background than the other sets presented, suggesting that the lower total metal content increases the probability of scattering of the incoming X-rays.

Discussion

Good correlations were found between the molarity of the elements in solution and the concentration obtained by using the portable ED-XRF over prepared discs. The lowest correlation coefficient (0.9555) and highest coefficient of variance (6%) were found for sulphur in set C, and all other are above 0.97 and below 4%. This minor discrepancy arises from the fact that sulphur has low sensitivity in XRF as the measured intensity at its $K\alpha$ energy

is significantly affected by background fluctuations. The $K\alpha$ of sulphur was not easily observed in the spectra of most standards of set C (Additional file 1: Fig. S4 from Online Resource). The occurrence of problems for the accurate quantification of sulphur in light matrixes was previously reported (Declercq et al. 2019) as well as for other light elements such as Al and Si in oils (Pedrozo-Peñafiel et al. 2019) and in ores (Zhou et al. 2020). In fact, this is quite difficult to achieve as this is a very insensitive element, and it is difficult to correct the background contribution within the limits of the tools provided by software.

In set B, it is observed in the spectra of the standards that the $L\alpha$ peak of praseodymium is not fully separated from its neodymium counterpart, rather appearing as a “shoulder” (Additional file 1: Fig. S3 from Online Resource), most likely because the pellets praseodymium content is much smaller than neodymium, contributing as well to increase the standard error of praseodymium calibration curve obtained by linear

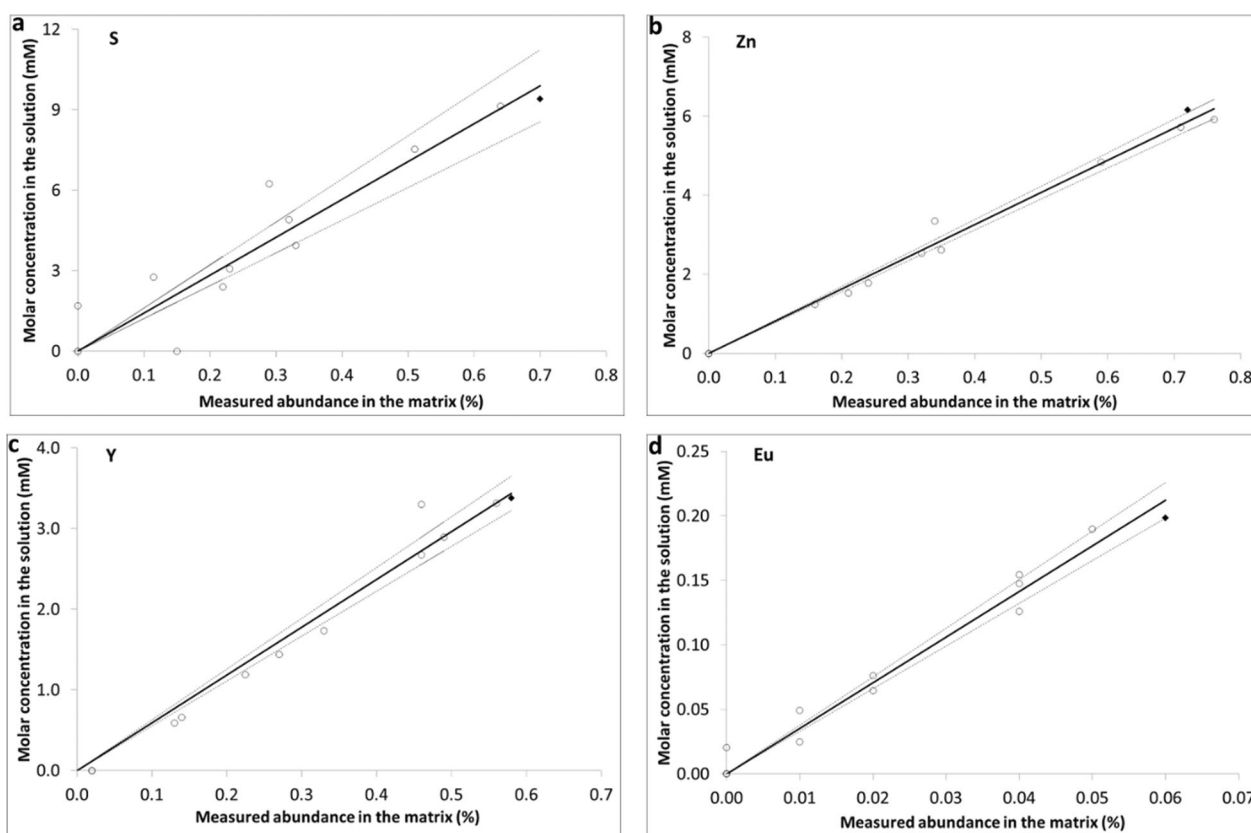


Fig. 4 Correlations obtained between metal concentration in solution and XRF measurements of the pellet, within set C elements (S, Zn, Y, Eu). The regression lines follow the equations: **a:** $S-y/mM = (14.14 \pm 0.88)x \%$, $R^2 = 0.9555$, $CV = 6\%$; **b:** $Zn-y/mM = (8.14 \pm 0.15)x \%$, $R^2 = 0.9961$, $CV = 2\%$; **c:** $Y-y/mM = (5.93 \pm 0.17)x \%$, $R^2 = 0.9905$ and a $CV = 3\%$; **d:** $Eu-y/mM = (3.54 \pm 0.11)x$, $R^2 = 0.9895$, $CV = 3\%$. The black diamond in each plot represents the standard that contains only the element of the respective curve

regression, comparing with the other elements, despite the good correlation found ($R^2 = 0.9772$, coefficient of variance = 4%, Fig. 3).

No strong matrix effects between elements were expected since the pressed pellets have low concentrations of the chosen elements and cellulose does not produce fluorescence. Nevertheless, interferences could occur among elements that possess an absorption edge very close to the emission energy of another element. To assess whether this effect could occur in each set, disc samples were prepared with only one of the studied elements. Results showed that in those pellets no such effects were observed. Although in some figures the diamond points were located outside their 95% confident interval, those points didn't fall always to the same side of the interval, suggesting a statistical dispersion of the experimental data. In addition, in the case of Y, from the two regression curves obtained at different concentrations, in only one of them the diamond point is outside, suggesting that samples with only one element have a similar behaviour when compared with the corresponding set, reinforcing that the matrix effects

are absent or minimal, as expected. Notwithstanding, matrix effects were still evaluated and some alpha coefficients were introduced in the spectrometer calibration (according to section "XRF specific calibrations") to correct any possible effects.

Intense background and Rayleigh scattering of the L lines of Rh were observed, namely in set C spectra (Additional file 1: Fig. S4 from Online Resource) as small concentrations of metals dispersed in a light matrix induce X-ray scattering, instead of good absorption.

The results obtained show that the two calibration curves for yttrium and zinc have different slopes in different sets. A slightly higher slope was estimated for higher concentrations of these elements, suggesting that for large ranges of composition the relation between the true value of composition in solution and the measure by ED-XRF is not linear and has a smooth curvature.

Taking into consideration the low volumes of samples used in this work, it is envisioned that small volumes (around 1 ml) are predictably enough to produce specimens to be analysed, which can constitute an advantage

of this methodology when a limited sample size is available. Nevertheless, if very concentrated solutions are to be analysed, different volumes may have to be used depending on the leachate sample levels.

The ED-XRF provides a robust analysis that can be employed as a quick or routine analytical methodology for liquid samples using a simple accessible pre-treatment and can be an alternative to more commonly employed spectroscopic analyses for solutions.

Conclusions

A simple methodology using a portable ED-XRF spectrometer to determine metal concentrations in solutions was presented. The equipment used is significantly cheaper, and the developed methodology has almost no operational costs when compared to other analytical techniques. Also, it is fast, does not require the use of vacuum or helium purges, is easily accessible, uses just common laboratory glassware and common innocuous chemicals and allows multi-elemental analysis in a row. The proposed simple methodology is therefore very convenient to analyse liquid samples, for instance, in industry and field works, where fast and easy to operate analyses are a necessary asset. The low volume required is an advantage if only a small sample is available. Although for higher concentrations the technique is more sensitive, this gain is small. Our analytical approach provided reliable and accurate results even when the emission peaks were not clearly observed in the spectra (Pr and S). Good correlations were obtained with a coefficient of determination not lower than 0.9555 and a coefficient of variance not above 6% for the three sets of chemical elements, including transition metals (Fe, Ni, Cu, Zn, Y), lanthanoids (Pr, Nd, Eu) and a non-metal (S). The methodology can be used for any sets of chemical elements detected by ED-XRF. However, in laboratories or industries where ED-XRF is not available or when, for instance, the analysis of very light elements is needed, the methodology may be used analogously with other compatible analytical techniques, such as LIBS and ion beam analysis, provided that appropriate calibrations are previously performed.

Supplementary Information

The online version contains supplementary material available at <https://doi.org/10.1186/s40543-024-00442-4>.

Additional file 1. Fig. S1. XRF spectrometer calibration curves for Fe, Pr and Nd solution (set B). Nd: $y=0.985x + 0.0017$, $R^2=0.9929$; Pr: $y=0.915x + 0.00014$, $R^2=0.9621$; Fe: $y=0.996x + 0.00017$, $R^2=0.9979$. **Fig. S2.** XRF spectrometer calibration curves for S, Zn, Y and Eu solution (set C). Y: $y=0.892x + 0.00038$, $R^2=0.9451$; Eu: $y=0.912x + 0.000033$, $R^2=0.9815$; Zn: $y=0.995x + 0.000045$, $R^2=0.9788$; S: $y=0.939x + 0.00018$, $R^2=0.9448$. **Fig. S3.** Spectrum from one standard regarding the Fe, Pr and Nd solution

(set B). **Fig. S4.** Spectrum from one standard regarding the S, Zn, Y and Eu solution (set C).

Acknowledgements

The authors are grateful to Dr. Maria Fátima Araújo (C²TN, IST, Lisboa) for insights into XRF interpretation.

Author contributions

JPL, FMJF and JS contributed to conceptualization; JPL and JS provided methodology and resources; FMJF and JMC performed investigation; FMJF performed writing (original draft preparation); FMJF, JMC, JPL and JS performed writing (review and editing); FMJF and JMC contributed to visualization; JPL and JS performed supervision. All authors have read and agreed to the published version of the manuscript.

Funding

This work was financially supported by Agência Nacional de Inovação Portugal (ANI) through project nº 33576 on the framework of co-promotion projects PT2020 and Fundação para a Ciência e Tecnologia, projects UIDB/00100/2020, UIDP/00100/2020 and LA/P/0056/2020. FMJF grateful acknowledges support from ANI and Instituto Superior Técnico—Universidade de Lisboa (IST-UL) for an individual research fellowship.

Availability of data and materials

Almost all details of experimental data are presented in the article or supplementary info.

Declarations

Competing interests

The authors declare no competing interests.

Author details

¹Centro de Recursos Naturais e Ambiente (CERENA), Instituto Superior Técnico, Universidade de Lisboa, Av. Rovisco Pais, 1, 1049-001 Lisbon, Portugal. ²Centro de Química Estrutural (CQE), Institute of Molecular Sciences (IMS), Instituto Superior Técnico, Universidade de Lisboa, Campus Tecnológico e Nuclear, Estrada Nacional 10, 2695-066 Bobadela, Lisbon, Portugal. ³Departamento de Engenharia e Ciências Nucleares (DECN), Instituto Superior Técnico, Universidade de Lisboa, Campus Tecnológico e Nuclear, Estrada Nacional 10, 2695-066 Bobadela, Lisbon, Portugal.

Received: 7 December 2023 Accepted: 22 April 2024

Published online: 07 May 2024

References

- Abrahami ST, Xiao Y, Yang Y. Rare-earth elements recovery from post-consumer hard-disc drives. *Miner Process Extr Metall Rev: Trans IMM* c. 2015;124(2):106–15. <https://doi.org/10.1179/1743285514Y.0000000084>.
- Akbulut S. Validation of classical quantitative fundamental parameters method using multivariate calibration procedures for trace element analysis in ED-XRF. *J Anal at Spectrom*. 2014;29(5):853–60. <https://doi.org/10.1039/C3JA50377A>.
- Binnemans K, Jones PT, Blanpain B, Gerven TV, Yang Y, Walton A, Buchert M. Recycling of rare earths: a critical review. *J Clean Prod*. 2013;51:1–22. <https://doi.org/10.1016/j.jclepro.2012.12.037>.
- Blotevogel S, Schreck E, Laplanche C, Besson P, Saurin N, Audry S, Viers J, Oliva P. Soil chemistry and meteorological conditions influence the elemental profiles of West European wines. *Food Chem*. 2019;298:125033. <https://doi.org/10.1016/J.FOODCHEM.2019.125033>.
- de la Calle I, Menta M, Klein M, Séby F. Screening of TiO₂ and Au nanoparticles in cosmetics and determination of elemental impurities by multiple techniques (DLS, SP-ICP-MS, ICP-MS and ICP-OES). *Talanta*. 2017;171:291–306. <https://doi.org/10.1016/j.talanta.2017.05.002>.
- Declercq Y, Delbecque N, De Grave J, De Smedt P, Finke P, Mouazen AM, Nawar S, Vandenberghe D, Van Meirvenne M, Verdoodt AA. Comprehensive

- study of three different portable XRF scanners to assess the soil geochemistry of an extensive sample dataset. *Remote Sens.* 2019;11(21):1–15. <https://doi.org/10.3390/rs11212490>.
- El-Taher A. Elemental analysis of granite by instrumental neutron activation analysis (INAA) and X-ray fluorescence analysis (XRF). *Appl Radiat Isot.* 2012;70(1):350–4. <https://doi.org/10.1016/J.APRAISO.2011.09.008>.
- European Commission, Directorate-General for Internal Market, Industry, Entrepreneurship and SMEs, *Report on critical raw materials and the circular economy*, Publications Office, 2018.
- Fiamegos Y, de la Calle Guntiñas MB. Validation strategy for an ed-xrf method to determine trace elements in a wide range of organic and inorganic matrices based on fulfilment of performance criteria. *Spectrochim Acta Part B: Spectrosc.* 2018;150(October):59–66. <https://doi.org/10.1016/j.sab.2018.10.009>.
- Fiamegos Y, Dumitrascu C, Ghidotti M, de la Calle Guntiñas MB. Use of energy-dispersive X-ray fluorescence combined with chemometric modelling to classify honey according to botanical variety and geographical origin. *Anal Bioanal Chem.* 2020;412(2):463–72. <https://doi.org/10.1007/S00216-019-02255-6>.
- Figueiredo FMJ, Araújo MF, Marçalo J, Leal JP, Sardinha JP. Determination of rare earth elements in CRT phosphors and NdFeB magnets residues using an ED-XRF portable spectrometer to assist field semi-quantitative screening. *Microchem J.* 2024;198:110136. <https://doi.org/10.1016/j.microc.2024.110136>.
- Fontàs C, Marguí E, Hidalgo M, Queralt I. Improvement approaches for the determination of Cr(VI), Cd(II), Pd(II) and Pt(IV) contained in aqueous samples by conventional XRF instrumentation. *X-Ray Spectrom.* 2009;38(1):9–17. <https://doi.org/10.1002/xrs.1093>.
- García-Florentino C, Maguregui M, Marguí E, Queralt I, Carrero JA, Madariaga JM. Development of X-ray fluorescence quantitative methodologies to analyze aqueous and acid extracts from building materials belonging to cultural heritage. *Anal Chem.* 2017;89(7):4246–54. <https://doi.org/10.1021/acs.analchem.7b00288>.
- Gentelli L. Chronological discrimination of silver coins based on inter-elemental ratios using laser ablation inductively coupled plasma mass spectrometry (LA-ICP-MS). *Archaeometry.* 2021;63(1):156–72. <https://doi.org/10.1111/ARCM.12628/FORMAT/PDF>.
- Gergoric M, Barrier A, Retegan T. Recovery of rare-earth elements from neodymium magnet waste using glycolic, maleic, and ascorbic acids followed by solvent extraction. *J Sustain Metall.* 2019;5(1):85–96. <https://doi.org/10.1007/s40831-018-0200-6>.
- Ghasemi J, Ahmadi S, Torkestani K. Simultaneous determination of copper, nickel, cobalt and zinc using zincon as a metallochromic indicator with partial least squares. *Anal Chim Acta.* 2003;487:181–8. [https://doi.org/10.1016/S0003-2670\(03\)00556-7](https://doi.org/10.1016/S0003-2670(03)00556-7).
- Goswami AP, Das S, Kalamdhad AS. Assessment of possible pollution risk using spatial distribution and temporal variation of heavy metals in river sediments. *Environ Earth Sci.* 2021;80(19):1–15. <https://doi.org/10.1007/S12665-021-09983-Y>.
- Hurst JA. Determination of soluble chromium(VI) in chromium plating mist by X-ray spectrometry. *Anal Chim Acta.* 1996;334(3):331–6. [https://doi.org/10.1016/S0003-2670\(96\)00352-2](https://doi.org/10.1016/S0003-2670(96)00352-2).
- Jenkins R, de Vries J. *Practical X-ray Spectrometry*. 2nd ed. Macmillan: London. 1973; ISBN: 978-1-349-00055-5
- Jha MK, Kumari A, Panda R, Kumar JR, Yoo K, Lee JY. Review on hydrometallurgical recovery of rare earth metals. *Hydrometallurgy.* 2016;165:2–26. <https://doi.org/10.1016/j.hydromet.2016.01.035>.
- Jin C. Clean chemistry for elemental impurities analysis of pharmaceuticals in compliance with USP 232. *AAPS Pharm Sci Tech.* 2016;17:1141–9. <https://doi.org/10.1208/s12249-015-0452-4>.
- Kalnicky DJ, Singhvi R. Field portable XRF analysis of environmental samples. *J Hazard Mater.* 2001;83(1–2):93–122. [https://doi.org/10.1016/S0304-3894\(00\)00330-7](https://doi.org/10.1016/S0304-3894(00)00330-7).
- Kejonen I, Haavisto O, Martikainen J, Suontaka V, Musuku B. Improving grade control efficiency with rapid on-line elemental analysis. *Miner Eng.* 2018;124:68–73. <https://doi.org/10.1016/J.MINENG.2018.05.002>.
- Lin EY, Rahmawati A, Ko JH, Liu JC. Extraction of yttrium and europium from waste cathode-ray tube (CRT) phosphor by subcritical water. *Pure Purif Technol.* 2018;2018(192):166–75. <https://doi.org/10.1016/j.seppur.2017.10.004>.
- Maione C, Araujo EM, Dos Santos-Araujo SN, Boim AGF, Barbosa RM, Alleoni LRF. Determining the geographical origin of lettuce with data mining applied to micronutrients and soil properties. *Sci Agric.* 2022;79(1):1–15. <https://doi.org/10.1590/1678-992X-2020-0011>.
- Maltsev AS, Ivanov AV, Pashkova GV, Marfin AE, Bishaev YA. New prospects to the multi-elemental analysis of single microcrystal of apatite by total-reflection X-ray fluorescence spectrometry. *Spectrochim Acta B: Spectrosc.* 2021;184:106281. <https://doi.org/10.1016/J.SAB.2021.106281>.
- Marguí E, Van Grieken R, Fontàs C, Hidalgo M, Queralt I. Preconcentration methods for the analysis of liquid samples by X-ray fluorescence techniques. *Appl Spectrosc Rev.* 2010;45(3):179–205. <https://doi.org/10.1080/05704920903584198>.
- Marguí E, Zawisza B, Sitko R. Trace and ultratrace analysis of liquid samples by X-ray fluorescence spectrometry. *TRAC Trends Anal Chem.* 2014;53:73–83.
- Miskufova A, Kochmanova A, Havlik T, Horvathova H, Kuruc P. Leaching of yttrium, europium and accompanying elements from phosphor coatings. *Hydrometallurgy.* 2018;2018(176):216–28. <https://doi.org/10.1016/j.hydromet.2018.01.010>.
- Morales J, Aguilera A, Bautista F, Cejudo R, Goguitchaichvili A, Hernández-Bernal MS. Heavy metal content estimation in the Mexico City Street dust: an inter-method comparison and Pb levels assessment during the last decade. *SN Appl Sci.* 2020. <https://doi.org/10.1007/s42452-020-03647-5>.
- Moriyama T, Morikawa A. Sample preparation for X-ray fluorescence analysis—VII. Liquid Sample. *Rigaku J.* 2017;33:24–9.
- Moriyasu K, Mizuta H, Nishikawa Y. Determination of rare-earth-metal ions by XRF with hydroxyiminodiacetic acid-chelating resin. *Bunseki Kagaku.* 1991;40(4):175–9. https://doi.org/10.2116/BUNSEKIKAGAKU.40.4_1757.
- Önal MAR, Binnemans K. Recovery of rare earths from waste cathode ray tube (CRT) phosphor powder by selective sulfation, roasting and water leaching. *Hydrometallurgy.* 2019;183:60–70. <https://doi.org/10.1016/j.hydromet.2018.11.005>.
- Önal MAR, Borra CR, Guo M, Blanpain B, Van Gerven T. Hydrometallurgical recycling of NdFeB magnets: complete leaching, iron removal and electrolysis. *J Rare Earths.* 2017;35(6):574–84. [https://doi.org/10.1016/S1002-0721\(17\)60950-5](https://doi.org/10.1016/S1002-0721(17)60950-5).
- Önal MAR, Riaño S, Binnemans K. Alkali baking and solvometallurgical leaching of NdFeB magnets. *Hydrometallurgy.* 2020;2020(191):105213. <https://doi.org/10.1016/j.hydromet.2019.105213>.
- Parhi PK, Sarangi K. Separation of copper, zinc, cobalt and nickel ions by supported liquid membrane technique using LIX 841, TOPS-99 and Cyanex 272. *Sep Purif Technol.* 2018;59:169–74. <https://doi.org/10.1016/j.seppur.2007.06.008>.
- Pathak AK, Kumar R, Singh VK, Agrawal R, Rai S, Rai AK. Assessment of LIBS for spectrochemical analysis: a review. *Appl Spectrosc Rev.* 2012;47:14–40. <https://doi.org/10.1080/05704928.2011.622327>.
- Pedrozo-Peñafliel MJ, Doyle A, Mendes LAN, Tristão MLB, Saavedra Á, Aucelio RQ. Methods for the determination of silicon and aluminum in fuel oils and in crude oils by X-ray fluorescence spectrometry. *Fuel.* 2019;243:493–500. <https://doi.org/10.1016/J.FUEL.2019.01.144>.
- Perring L, Andrey D. Multi-elemental ED-XRF determination in dehydrated bouillon and sauce base products. *Food Anal Methods.* 2018;11(1):148–60. <https://doi.org/10.1007/S12161-017-0985-0>.
- Perring L, Nicolas M, Andrey D, Fragnière Rime C, Richoz-Payot J, Dubascoux S, Poitevin E. Development and validation of an ED-XRF method for the fast quantification of mineral elements in dry pet food samples. *Food Anal Methods.* 2017;10(5):1469–78. <https://doi.org/10.1007/S12161-016-0695-Z>.
- Pinheiro FC, Barros I, Nóbrega JA. Elemental impurities analysis in name-brand and generic omeprazole drug samples. *Heliyon.* 2020. <https://doi.org/10.1016/J.HELIYON.2020.E03359>.
- Pinho SC, Ribeiro C, Ferraz CA, Almeida MF. Copper, zinc, and nickel recovery from printed circuit boards using an ammonia-ammonium sulphate system. *J Mater Cycles Waste Manag.* 2021;23:1456–65. <https://doi.org/10.1007/s10163-021-01226-3>.
- Pinjun L, Zhengye X, Zidong M, Jingyuan G, Chunxi W. Analysis of Cu and Zn contents in aluminum alloys by femtosecond laser-ablation spark induced breakdown spectroscopy. *Open Phys.* 2023;21:20230113. <https://doi.org/10.1515/phys-2023-0113>.
- Popp M, Hann S, Koellensperger G. Environmental application of elemental speciation analysis based on liquid or gas chromatography hyphenated

- to inductively coupled plasma mass spectrometry—a review. *Anal Chim Acta*. 2010;668(2):114–29. <https://doi.org/10.1016/j.aca.2010.04.036>.
- Potts PJ, Webb PC, Watson JS. Silicate rock analysis by energy-dispersive X-ray fluorescence using a cobalt anode X-ray tube: Part I. Optimisation of excitation conditions for chromium, vanadium, barium and the major elements. *J Anal at Spectrom*. 1986;1(4):467–71. <https://doi.org/10.1039/JA9860100467>.
- Pozebon D, Scheffler GL, Dressler VL. Elemental hair analysis: a review of procedures and applications. *Anal Chim Acta*. 2017;992:1–23. <https://doi.org/10.1016/J.ACA.2017.09.017>.
- Ray AR, Mishra S. Hydro metallurgical technique as better option for the recovery of rare earths from mine tailings and industrial wastes. *Sustain Chem Pharm*. 2023;36:101311. <https://doi.org/10.1016/j.scp.2023.101311>.
- Riding JB. A guide to preparation protocols in palynology. *Palynology*. 2021;45(S1):1–110. <https://doi.org/10.1080/01916122.2021.1878305>.
- Rodrigues ARN, Melquiades FL, Appoloni CR, Marques EN. Characterization of Brazilian banknotes using portable X-ray fluorescence and Raman spectroscopy. *Forensic Sci Int*. 2019;302:109872.
- Rodushkin I, Engström E, Baxter DC. Sources of contamination and remedial strategies in the multi-elemental trace analysis laboratory. *Anal Bioanal Chem*. 2010;396:365–77. <https://doi.org/10.1007/s00216-009-3087-z>.
- Rowe H, Hughes N, Robinson K. The quantification and application of handheld energy-dispersive x-ray fluorescence (ED-XRF) in mudrock chemostratigraphy and geochemistry. *Chem Geol*. 2012;324–325:122–31. <https://doi.org/10.1016/j.chemgeo.2011.12.023>.
- Rudovica V, Viksna A, Actins A. Application of LA-ICP-MS as a rapid tool for analysis of elemental impurities in active pharmaceutical ingredients. *J Pharm Biomed Anal*. 2014;91:119–22. <https://doi.org/10.1016/JJPBA.2013.12.025>.
- Shah R, Devi S. Chelating resin containing s-bonded dithizone for the separation of copper(II), nickel(II) and zinc(II). *Talanta*. 1998;45:1089–96. [https://doi.org/10.1016/S0039-9140\(97\)00215-4](https://doi.org/10.1016/S0039-9140(97)00215-4).
- Shinn AP, Bron JE, Gray DJ, Sommerville C. Elemental analysis of Scottish populations of the ectoparasitic copepod *Lepeophtheirus salmonis*. *Contrib Zool*. 2000;69(1–2):79–87. <https://doi.org/10.1163/18759866-0690102009>.
- Skoog DA, Holler, FJ, Crouch, SR. *Principles of Instrumental Analysis*. 7th ed. Cengage Learning. 2017.
- Sokolova LP, Skorniyakov VV, Kargman VB, Saldadse KM. Selective Separation of components [copper, nickel, zinc, chromium(VI)] in the process of ion-exchange purification of wastewaters. *J Chromatogr A*. 1986;364:135–42. [https://doi.org/10.1016/S0021-9673\(00\)96203-4](https://doi.org/10.1016/S0021-9673(00)96203-4).
- Sysoev AA. Mass-spectrometric elemental analysis of solid substances in Russia. *J Anal Chem*. 2011;66(11):1079–89. <https://doi.org/10.1134/S106193481111013X>.
- Teixeira LSG, Rocha RBS, Sobrinho EV, Guimarães PRB, Pontes LAM, Teixeira JSR. Simultaneous determination of copper and iron in automotive gasoline by X-ray fluorescence after pre-concentration on cellulose paper. *Talanta*. 2007;72(3):1073–6. <https://doi.org/10.1016/J.TALANTA.2006.12.042>.
- Williams R, Taylor G, Orr C. pXRF method development for elemental analysis of archaeological soil. *Archaeometry*. 2020;62(6):1145–63. <https://doi.org/10.1111/ARCM.12583>.
- Yin X, Tian X, Wu Y, Zhang Q, Wang W, Li B, Gong Y, Zuo T. Recycling rare earth elements from waste cathode ray tube phosphor: experimental study and mechanism analysis. *J Clean Prod*. 2018;205:58–66. <https://doi.org/10.1016/j.jclepro.2018.09.055>.
- Zhang ZX, Li YR, Liu RT, Chen ZX, Weng LH, Zhou XG. Insertion reaction of elemental sulfur into the Ln–C bond: synthesis and characterization of [(C₅H₄SiMe₂tBu)₂Ln(μ-SR)]₂ (R = Me, Ln = Yb, Er, Dy, Y; R = ⁿBu, Ln = Yb, Dy). *Polyhedron*. 2007;26(17):4986–92. <https://doi.org/10.1016/J.POLY.2007.07.010>.
- Zhou FB, Li CG, Zhu HQ, Li YG. A novel method for simultaneous determination of zinc, nickel, cobalt and copper based on UV-vis spectrometry. *Optik*. 2019;182:58–64. <https://doi.org/10.1016/j.ijleo.2018.12.159>.
- Zhou S, Yuan Z, Cheng Q, Weindorf DC, Zhang Z, Yang J, Zhang X, Chen G, Xie S. Quantitative analysis of iron and silicon concentrations in iron ore concentrate using portable X-ray fluorescence (XRF). *Appl Spectrosc*. 2020;74(1):55–62. <https://doi.org/10.1177/0003702819871627>.

Publisher's Note

Springer Nature remains neutral with regard to jurisdictional claims in published maps and institutional affiliations.